Bioresource Technology 435 (2025) 132873

Contents lists available at ScienceDirect

Bioresource Technology

journal homepage: www.elsevier.com/locate/biortech

Impact of light intensity on purple phototrophic bacteria mixed cultures: experimental insights and biokinetic modelling

Ali Amini [a], Simone Rossi [a], Valiallah Amirian Mojarad [a], Gabriele Bellotti [b], Fabrizio Cappa [b], Filippo Vaccari [b], Edoardo Puglisi [b], Roberto Canziani [a], Elena Ficara [a], Andrea Turolla [a,*]

[a] Department of Civil and Environmental Engineering (DICA), Politecnico di Milano, Piazza Leonardo da Vinci 32, 20133 Milan, Italy
[b] Department of Sustainable Food Process (DISTAS), Faculty of Agricultural, Food and Environmental Sciences, Università Cattolica del Sacro Cuore, Piacenza, Italy

HIGHLIGHTS

- Light intensity effect (10–60 $W \cdot m^{-2}$) on the growth kinetics of a mixed PPB culture.
- Development and calibration of a simplified PPB growth model with acetate uptake.
- Microbial characterization of the mixed culture under different growing conditions.
- Model validation and scenario analysis for supporting flat-plate PBR design.

GRAPHICAL ABSTRACT

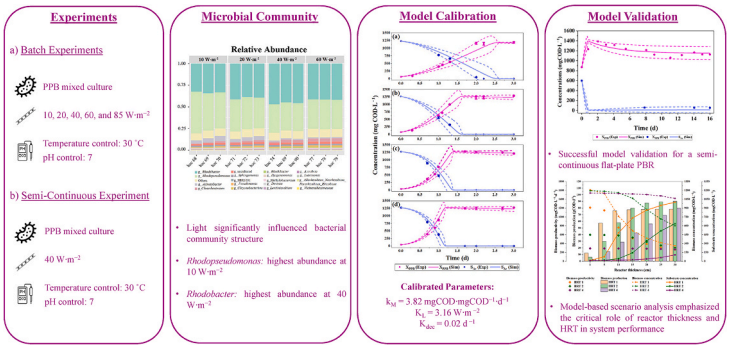

ARTICLE INFO

Keywords:
Phototrophic microorganisms
Photobioreactors
Parameter estimation
Model validation
Optimal growth conditions
Model-based scenario analysis

ABSTRACT

Developing kinetic models is crucial for understanding and optimizing purple phototrophic bacteria (PPB) growth in photobioreactors (PBR). Given the significant role of radiation transfer, integrating light into PPB kinetic models is fundamental for enhancing PBR design and operation. In this study, batch experiments were conducted under monochromatic light intensity conditions ranging from 10 to 60 $W \cdot m^{-2}$ to assess the influence of this parameter on a mixed PPB culture. An existing biokinetic model was adapted to incorporate the light dependence of PPB growth using a Monod-type light function, which included light attenuation based on experimentally measured mass extinction coefficients. Microbiological characterizations evidenced the selective pressure of light on the PPB mixed culture, and the developed model could effectively describe the population behavior. Estimated parameters were validated in a continuous PBR operated at 40 $W \cdot m^{-2}$, demonstrating the model ability to predict biomass growth and substrate consumption, and to support technological upscaling.

* Corresponding author.
E-mail address: andrea.turolla@polimi.it (A. Turolla).

https://doi.org/10.1016/j.biortech.2025.132873
Received 26 October 2024; Received in revised form 7 June 2025; Accepted 21 June 2025
Available online 22 June 2025

1. Introduction

Purple phototrophic bacteria (PPB) are gaining significant attention in the fields of environmental and industrial biotechnology due to their outstanding potential for resource recovery. PPB can sustainably produce valuable bioproducts such as single-cell proteins, biohydrogen, polyhydroxyalkanoates, natural pigments (Capson-Tojo et al., 2020), while simultaneously removing nutrients from different waste streams (Hülsen et al., 2014; Kaewsuk et al., 2010; Liu et al., 2015; Prachanurak et al., 2014).

Optimizing growth conditions is crucial in exploiting PPB-based biotechnologies, given their high capital and operational costs (Capson-Tojo et al., 2020). To optimize cultivation conditions by the appropriate design and operation of photobioreactors (PBR), it is essential to use mathematical models, as they help to understand PPB growth dynamics and to fine-tune cultivation parameters under various environmental conditions (Capson-Tojo et al., 2023; Cerruti et al., 2022; Puyol et al., 2017).

Nevertheless, predicting PPB growth presents several challenges, mainly due to the dependence of involved biological phenomena on various factors, including the availability of light and nutrients (Capson-Tojo et al., 2023; Puyol et al., 2017). While significant progress has been made in modelling phototrophic microorganisms, mainly microalgae (Casagli et al., 2021; Solimeno et al., 2015), these models cannot be directly applied to PPB due to key differences (Rossi et al., 2025). For example, PPB absorb over a broader radiative spectrum, including near-infrared (NIR) and visible light, but exhibit higher water-selective absorption in the NIR range compared to microalgae (Capson-Tojo et al., 2022).

Mathematical modelling is widely employed in the context of bioprocess engineering to quantify the relationships between the specific growth rate and different environmental factors (Lee et al., 2015). While many of the existing mathematical models for PPB growth have primarily aimed at describing the metabolic pathways in pure cultures (Golomysova et al., 2010; Hädicke et al., 2011; Tec-Campos et al., 2023), these metabolic models are especially complex, with many equations and parameters, which makes them unsuitable for process control and simulation in wastewater treatment. Instead, Monod-type models offer a simpler approach to describe the dependence of the specific growth rate on the concentrations of limiting nutrients and have been successfully applied to PPB mixed cultures (Dalaei et al., 2020).

The development of Monod-type biochemical models for wastewater treatment by PPB was first introduced by Puyol et al. (2017), who proposed the photo-anaerobic model (PAnM). This model describes the growth of PPB in wastewater but does not account for microbial competition and assumes constant light intensity throughout the modelling phase without considering light attenuation. However, as thoroughly discussed by Amini et al. (2025), increasing biomass concentration leads to light attenuation, and as light penetrates the medium, attenuation further reduces light intensity with increasing light path. To address these issues, Capson-Tojo et al. (2023) introduced the extended photo-anaerobic model (e-PAnM), aiming to account for the co-existence of different microorganisms and light attenuation for flat-plate PBRs. Alloul et al. (2023) further improved this approach for PPB mixed cultures, integrating three PPB metabolisms with competing aerobic and anaerobic organisms in a raceway PBR.

In the case of phototrophic microorganisms such as PPB or microalgae, the effect of available light intensity must be carefully considered and modelled locally in PBRs (Martínez et al., 2018). For microalgae, previous research works have shown that when the light intensity is lower than the saturation level, the growth rate is reduced by the light availability due to light limitation (Carvalho et al., 2011). Conversely, when the light intensity exceeds the optimal (saturation) level, it strongly hinders the phototrophic metabolisms due to photo-inhibition phenomena (Bernard and Rémond, 2012). However, concerning research works on PPB, photo-inhibition has been only reported for PPB pure cultures in a few research studies. Ross and Pott (2022) explored the effect of different light intensities ranging from 30 to 600 $W{\cdot}m^{-2}$ on *Rhodopseudomonas palustris* using a polychromatic light source. The results indicated that the culture experienced photo-limitation below 200 $W{\cdot}m^{-2}$ and photo-inhibition above 600 $W{\cdot}m^{-2}$. Zhou et al. (2014) found that *Rhodopseudomonas* biomass increased with light intensities between 500 and 2000 lx (~ 3.9–15.8 $W{\cdot}m^{-2}$), but declined with increasing light intensity to 8000 lx (~ 63.2 $W{\cdot}m^{-2}$) due to photo-inhibition. Similarly, Shi and Yu (2005) reported higher biomass of *Rhodopseudomonas capsulata* at 2000–4000 lx (~ 15.8–31.6 $W{\cdot}m^{-2}$), with a notable decline above 5000 lx (~ 39.5 $W{\cdot}m^{-2}$). It must be emphasized that comparisons based solely on lux values, particularly between pure cultures illuminated with visible light and mixed cultures requiring NIR spectra, may be biased or misleading. Notably, photoinhibition has not yet been observed for PPB mixed cultures, which may be attributed to the acclimation potential of mixed cultures to high light intensities.

Therefore, to develop an accurate modelling framework for the influence of light intensity on PPB mixed cultures and potential photo-inhibition, lab-scale experiments were conducted in the present work to investigate the effects of different light intensities on microbial community and growth kinetics of a mixed PPB culture fed with acetate. Experimental data were then used to develop a modified version of existing biokinetic models, embedding the description of light attenuation with a Monod-type light limiting function. Finally, the parameters obtained from batch experiments were validated using a semi-continuous PBR at 40 $W{\cdot}m^{-2}$. The ultimate goal of the present work is to support the development of reliable tools for PPB mixed cultures modelling, representing a step towards technological upscaling.

2. Materials and methods

2.1. Enrichment reactor and growth medium for purple phototrophic bacteria

The experiments were conducted using an inoculum containing a mixed culture of PPB, which was enriched from an environmental sample collected from a pond in a peri-urban wetland in the Milan area (Northern Italy). The enrichment process was performed under anaerobic conditions in a 5.6-L cylindrical reactor, in which the pH level was adjusted to 7.0 ± 0.1 and the temperature was kept at 30 ± 1 ℃ via a cooling pipe around the external reactor surface. The reactor was magnetically stirred at approximately 350 RPM and illuminated with monochromatic LED strips (Waveform Lighting) with a peak wavelength at 850 nm, attached to the external surface of the reactor. The reactor was encased in a dark box to prevent the penetration of environmental light. The growth medium for enrichment and cultivation was based on a modified Ormerod medium (Ormerod et al., 1961). The modification was based on Delamare-Debouteville et al. (2019), in which biotin, ammonium sulfate, and malic acid were substituted with yeast extract (0.015 $mg{\cdot}L^{-1}$), ammonium chloride (150 $mg{\cdot}L^{-1}$), and sodium acetate (1300 mg $COD{\cdot}L^{-1}$), respectively. The enrichment reactor was operated semi-continuously, with two-thirds of the reactor volume replaced every week with the same amount of fresh modified Ormerod medium, resulting in an average hydraulic retention time (HRT) of 10.5 d.

2.2. Batch growth tests

Batch experiments were performed in lab-scale flat-plate PBRs constituted by rectangular cell culture flasks made of transparent polystyrene. The flasks had a maximum volume of 316.5 mL, a surface area of 75 cm^2, a flask thickness of 3.3 cm, a wall thickness of 1.5 mm with a total light transmittance of 90 %. They were completely filled to avoid any headspace. The growth medium was first introduced into the flask, then the PPB inoculum was added, reaching the maximum flask volume and resulting in an initial biomass concentration of 35–74 mg $COD{\cdot}L^{-1}$. The flasks were subsequently closed with plug-seal caps and

continuously mixed at approximately 350 RPM by magnetic stirring bars. Although mixing efficiency can be limited with this configuration, high rotation speed was applied to approximate ideal mixing. In addition, while the presence of a plug seal is fundamental for maintaining anaerobic conditions, the absence of headspace in the system can lead to changes in the partial pressures of CO_2 or other gases due to bacterial consumption or production. Nevertheless, this type of setup is considered suitable for PPB growth tests, and given the short duration of the experiments, gas production or consumption was considered negligible. This assumption is further supported by Capson-Tojo et al. (2023), who reported that only $5.2{\cdot}10^{-7}$ g CO_2-C·g COD^{-1}-acetate is produced under anaerobic conditions. Batch experiments were carried out under different monochromatic (850 nm) incident light intensities of 10, 20, 40, and 60 W·m^{-2}. Moreover, to further assess the potential occurrence of photo-inhibition at higher light intensities, an additional batch experiment was conducted at 85 W·m^{-2}. The irradiation was provided from one side of the flasks by the same LED strips used for the enrichment reactor, with the light intensity continuously monitored with a radiometer (International Light, ILT 1400) at the front wall of the flasks. The experiments were conducted in triplicate in an opaque black box to avoid interferences due to the ambient light penetration. The temperature was kept constant and homogeneous at 30 ± 2 °C thanks to a cooling and a recirculation fan, and pH was adjusted to remain within the range of 6.8–7.2.

The tested range of light intensities is particularly relevant when considering natural sunlight conditions. On a clear day at sea level, the maximum solar irradiance is approximately 1000 W·m^{-2}. Despite the NIR spectrum accounts for about 28 % of the total solar spectrum at the Earth's surface (approximately 280 W·m^{-2}) (Collins et al., 2006), PPB do not absorb across the entire NIR range, which extends up to 2500 nm. Instead, their light-harvesting complexes can absorb within the 800–900 nm range. In this study, illumination was applied at 850 nm that lies within the peak absorption range. Moreover, various factors can contribute to the attenuation of sunlight, further reducing the maximum NIR irradiance from solar radiation on a clear day. For instance, atmospheric scattering can reduce direct beam and diffuse light by around 17 %, with this effect increasing by up to an additional 30 % depending on latitude. Adverse weather conditions, such as cloud cover, can cause a further 65 % reduction in irradiance compared to clear sky conditions. Additionally, the orientation of the culture relative to the sun can result in up to a 50 % decrease in the received light intensity (Damergi et al., 2021). These factors mean that, in many real-world scenarios, the light intensity experienced by PBRs is significantly lower than the theoretical maximum (for example, based on above calculations, the overall NIR intensity would typically range from 28 to 163 W·m^{-2}, under different conditions).

2.3. Flat-plate photobioreactor in semi-continuous mode

In view of model validation, an additional experiment was conducted in continuous mode using a 10-L flat-plate PBR (40 × 40 × 7 cm), illuminated from one side with an average incident light intensity of 40 W·m^{-2} at the wall by means of 4 monochromatic lamps (96 LED array, 12 W electric power each) at a wavelength of 850 nm. The PBR was covered with UV–VIS absorbing foil (ND 1.2 299, Transformation Tubes) to prevent the ambient light from non-NIR wavelengths. The PBR was first inoculated from the 5-L reactor and enriched in batch mode. Subsequently, the PBR was operated for a duration of 16 d (in semi-continuous mode) and maintained under steady-state conditions. The HRT was maintained at 4 d, and the organic loading rate (OLR) was 0.317 g COD·L^{-1}·d^{-1}. Although the HRT and OLR were relatively high and low, respectively, they fall within the typical ranges reported in the literature for PPB systems (Capson-Tojo et al., 2020; García et al., 2019; Liu et al., 2016). The feeding was based on the same modified Ormerod medium, ensuring an adequate supply of nutrients for PPB growth. Throughout the experiment, the temperature was maintained at 30 ± 1 °C, while the pH was continuously controlled at 7.0 ± 0.1 by adding HCl (3 M).

2.4. Analytical methods

Samples extracted from the flasks and PBR were immediately analyzed to measure temperature, pH, nitrogen concentrations, soluble COD (sCOD) and total COD of pelleted biomass. Temperature and pH were measured with a handheld multi-parametric device (Hach Lange, HQ40d). The nitrogen and sCOD concentrations, after membrane filtration (0.45-μm cutoff), were measured with spectrophotometric test kits (Hach, LCK314 and LCK303, respectively). Moreover, the total COD of biomass, after centrifugation at 15,000 rpm in 2-mL Eppendorf tubes and removal of the supernatant, was measured with spectrophotometric test kits (Hach, LCK514). Biomass yields (Y) for each batch experiment were calculated based on the initial and final measured biomass concentrations and sCOD (in COD units) as shown in Eq. (1).

$$Y = \frac{biomass\ \ concentration_{final} - biomass\ \ concentration_{initial}}{sCOD_{initial} - sCOD_{final}} \quad (1)$$

2.5. Microbial community characterization

At the end of the batch experiments, samples from each test were collected to assess the impact of different light intensities on the microbial community structure. Samples from each test were processed in triplicate. Total DNA was extracted with the FastDNA™ SPIN Kit for Soil (MP Biomedicals, Santa Ana, CA, USA) according to the manufacturer's protocol starting from 500 μL of bacterial suspension. The hypervariable 16S V3-V4 region was targeted and PCR-amplified. Each PCR mixture consisted of 12.5 μL of Phusion Flash High-Fidelity Master Mix (Thermo Fisher Scientific), 1.25 μL of both forward and reverse primers (10 μM), 1 ng of DNA template, and nuclease-free water, with a total volume of 25 μL. The universal primers used were 343f (5′-TACGGRAGGCAGCAG-3′) and 802r (5′-TACNVGGGTWTCTAATCC-3′) (White et al., 1990). The thermal cycling protocol included an initial denaturation at 95 °C for 5 min, followed by 20 cycles of denaturation at 95 °C for 30 s, annealing at 50 °C for 30 s, extension at 72 °C for 30 s, and a final extension at 72 °C for 10 min. A nested PCR approach was used, with the products from the first PCR serving as templates for a second amplification step (Berry et al., 2011). The forward primers in the second PCR were indexed with a 9-base extension at their 5′ end. The products from the second amplification were pooled into a single multiplexed sample, with 30 ng of DNA per sample. The pooled products were purified using the solid-phase reversible immobilization (SPRI) method (Agencourt AMPure XP kit; REF A63880, Beckman Coulter). The sequencing was carried out by Novogene UK, with amplicon library preparation performed using the TruSeq DNA sample preparation kit (REF 15026486, Illumina Inc.). Sequencing was completed on the Novaseq 6000 Illumina platform, generating 250 bp paired-end reads.

Illumina barcode demultiplexing and base calling were performed using MiSeq Control Software version 2.3.0.3, RTA v1.18.42.0, and CASAVA v1.8.2. Raw sequences were aligned using the pandaseq script (Bartram et al., 2011), with a minimum overlap of 30 bp between paired reads and a maximum allowance of two mismatches. After filtering, trimming, and denoising the demultiplexed sequences for each sample, chimeric sequences were identified and removed using the QIIME™ 2 vsearch plugin. The QIIME™ 2 feature-classifier plugin was then used to align the ASV sequences with a pre-trained Silva database, which was used to produce the taxonomy table. Downstream statistical analyses carried out on microbiome data were performed with the pipelines provided in Microbiome Analyst v2.0 (Lu et al., 2023). Raw amplicon sequencing reads were deposited in the NCBI Sequence Read Archive (SRA) under BioProject accession number PRJNA1256429. Individual run accession numbers are available under SRA accessions SAMN48179479-SAMN48179490.

2.6. Model description

Experimental data from batch growth tests for PPB and substrate concentrations were modelled as a mixed reactor compartment with constant volume with the AQUASIM 2.0 software (Reichert, 1994). The Monod-type biochemical model developed in this work was obtained by implementing a simplified version of the PAnM model (Puyol et al., 2017). To accurately represent the phenomena expected in batch experiments while reducing the model complexity, the growth of PPB was simulated by considering only three processes, namely hydrolysis of particulate organic matter, acetate uptake by PPB, and PPB decay. In this model, a substrate half-saturation constant (K_S) and a hydrolysis first order constant (k_{hyd}) of 20 mg COD·L^{-1} and 0.07 d^{-1} were assumed, respectively (Puyol et al., 2017). Moreover, the experimentally measured biomass yields under different light intensity conditions were used for the model. The Petersen matrix for the model and the reference values for stoichiometric coefficients and kinetic parameters, assumed as in the PAnM, are reported in Table 1 and Table 2, respectively. The most relevant model parameters were dynamically estimated by simultaneously calibrating the model against experimental data from the four batch tests conducted under different light intensities. This was achieved using the "calculation number" program variable in AQUASIM. The parameters selected for calibration were based on the outcomes of the sensitivity analysis described in Section 2.7.

The dependence of acetate uptake by PPB on light intensity was modelled based on the Monod-type function (Capson-Tojo et al., 2022), as shown in Eq. (2).

$$k_{M,I} = K_M \cdot \left(\frac{I_{ave}}{I_{ave} + K_L} \right) \tag{2}$$

where $k_{M,I}$ (mg COD·mg COD^{-1}·d^{-1}) is the specific uptake rate, k_M (mg COD·mg COD^{-1}·d^{-1}) is the maximum specific uptake rate, I_{ave} (W·m^{-2}) is the average light intensity, and K_L (W·m^{-2}) is the light half-saturation coefficient.

Considering light attenuation is essential, as neglecting this phenomenon throughout the reactor would prevent the model from accounting for this effect in the PBR, thereby overlooking a crucial factor (Amini et al., 2025; Capson-Tojo et al., 2023; Casagli et al., 2021). Light attenuation due to the presence of the concentrated PPB suspension throughout the reactor depth was evaluated according to the Beer-Lambert law (Eq. (3)), which was integrated along the reactor depth to determine the average light intensity (Eq. (4)).

$$I(z) = I_0 \cdot \exp(-\varepsilon \cdot X_{PPB} \cdot z) \tag{3}$$

$$I_{ave} = \frac{1}{L} \int_0^L I(z) \cdot dz \tag{4}$$

where I_z (W·m^{-2}) is the light intensity at depth z (m), I_0 (W·m^{-2}) is the incident light intensity, X_{PPB} (mg COD·L^{-1}) is the PPB biomass concentration, and L (m) is the total light path.

In Eq. (3), the mass extinction coefficients (ε) (see Supplementary Material) were estimated through dedicated experiments in our previous work for the same incident light intensities, which demonstrated that these coefficients, although independent of the biomass concentrations, exhibited different values at different light intensities and were used as variable inputs for the model (Amini et al., 2025). This is in contrast with the results of Capson-Tojo et al. (2022), who estimated these coefficients mathematically through curve fitting and concluded that they were dependent on the biomass concentration.

In terms of nutrient dependency, given the presence of nutrient excess conditions for nitrogen and phosphorus, the only limiting factor that was taken into consideration was for acetate (S_{AC}), as shown in Eq. (5). For this model component, Monod-type expression was used, consistently with previous literature works available for PPB (Capson-Tojo et al., 2023; Puyol et al., 2017).

Table 1
Petersen matrix of the proposed model.

Component →	i	1	2	3	4	5	6	7	8	9	10	Process rate
j	Process ↓	S_s	S_{AC}	S_{IC}	S_{H2}	S_{IN}	S_{IP}	S_I	X_{PPB}	X_S	X_I	
1	Phototrophic acetate uptake by PPB	0	−1	$f_{IC,ph,AC}$	0	$-f_{N,B}$	$-f_{P,B}$	0	1	0	0	$r_{ph} = k_{M,I} \cdot F_S \cdot F_N \cdot F_P \cdot X_{PPB}$
2	Hydrolysis	$f_{SS,xs}$	$f_{SAC,xs}$	$f_{IC,xs}$	$f_{H2,xs}$	$f_{IN,xs}$	$f_{IP,xs}$	$f_{SI,xs}$	0	−1	$f_{XI,xs}$	$r_{hyd} = k_h \cdot X_s$
3	Decay of X_{PPB}	0	0	$f_{C,B}-f_{C,xs}$	0	$f_{N,B}-f_{N,xs}$	$f_{P,B}-f_{P,xs}$	0	−1	1	0	$r_{dec} = k_{dec} \cdot X_{PPB}$
State variables		Biodegradable soluble fraction but acetate (mg COD·L^{-1})	Acetate (mg COD·L^{-1})	Inorganic carbon (mol C·L^{-1})	Hydrogen as COD (mg COD·L^{-1})	Inorganic nitrogen as ammonia (mg N·L^{-1})	Inorganic phosphorus as phosphate (mg P·L^{-1})	Soluble inerts (mg COD·L^{-1})	PPB biomass (mg COD·L^{-1})	Organic biodegradable particulate (mg COD·L^{-1})	Particulate inerts (mg COD·L^{-1})	**Inhibition functions** $F_S = \frac{S_{AC}}{K_S + S_{AC}}$ $F_N = \frac{S_{IN}}{K_{S,IN} + S_{IN}}$ $F_P = \frac{S_{IP}}{K_{S,IP} + S_{IP}}$

Table 2
Stochiometric coefficients and kinetic parameters used for the model assumed as in the PAnM by Puyol et al. (2017).

Symbol	Parameter	Value (±standard error)
$f_{SS,xs}$	Soluble substrate production but acetate in hydrolysis (mg COD·mg COD^{-1})	0.164
$f_{SAC,xs}$	Acetate production in hydrolysis (mg COD·mg COD^{-1})	0.167
$f_{IC,ph,AC}$	Inorganic carbon production from acetate in photoheterotrophy (mol C·mg COD^{-1})	6.45E-6
$f_{IC,xs}$	Inorganic carbon production in hydrolysis (mol C·mg COD^{-1})	1.30E-6
$f_{H2,xs}$	Hydrogen production in hydrolysis (mg COD·mg COD^{-1})	0.084
$f_{IN,xs}$	Ammonia production in hydrolysis (mg N·mg COD^{-1})	0.016
$f_{IP,xs}$	Phosphate production in hydrolysis (mg P·mg COD^{-1})	0.003
$f_{SI,xs}$	Soluble inert production in hydrolysis (mg COD·mg COD^{-1})	0.15
$f_{XI,xs}$	Particulate inert production in hydrolysis (mg COD·mg COD^{-1})	0.43
$f_{N,B}$	Nitrogen content of PPB (mg N·mg COD^{-1})	0.086
$f_{P,B}$	Phosphorus content of PPB (mg N·mg COD^{-1})	0.015
$f_{C,B}$	Carbon content of PPB (mol C·mg COD^{-1})	2.48E-5
$f_{C,xs}$	Carbon content of biodegradable particulate (mol C·mg COD^{-1})	2.50E-5
$f_{N,xs}$	Nitrogen content of biodegradable particulate (mg N·mg COD^{-1})	0.028
$f_{P,xs}$	Phosphorus content of biodegradable particulate (mg P·mg COD^{-1})	0.005
k_{hyd}	Hydrolysis first order constant (d^{-1})	0.071 ± 0.002
k_M	Specific uptake rate for acetate (mg COD·mg COD^{-1}·d^{-1})	2.4 ± 0.1
K_S	Saturation constant for acetate in photoheterotrophy (mg COD·L^{-1})	20 ± 4
$K_{S,IN}$	Saturation constant for inorganic nitrogen assimilation (mg N·L^{-1})	0.02 ± 0.05
$K_{S,IP}$	Saturation constant for inorganic phosphorus assimilation (mg P·L^{-1})	0.081 ± 0.005
k_{dec}	Biomass decay (d^{-1})	0.09 ± 0.02
Y	Biomass yield (mg COD·mg COD^{-1})	1 ± 0.03

$$F_{AC} = \left(\frac{S_{AC}}{S_{AC} + K_S}\right) \tag{5}$$

where F_{AC} is the limiting function for acetate and K_S is the acetate half-saturation coefficient.

2.7. Sensitivity analysis, parameter identification, and quality of fit

A sensitivity analysis was performed using the dedicated AQUASIM toolbox, which allowed the identification of the most influential parameters on model outputs. The absolute-relative function (δ_{yp}^{ar}) was used, as reported in Eq. (6).

$$\delta_{yp}^{ar} = p\frac{\partial y}{\partial p} \tag{6}$$

where p is the parameter and y is a model variable.

Parameter identification involved those parameters that were identified as most sensitive by the sensitivity analysis. The calibration was carried out on biomass and substrate concentrations (without providing weights), and parameters that were not subjected to calibration were kept at their nominal value, as reported in previous relevant modelling studies (see Table 2). As for experimental data, each triplicate measure was processed as an individual data point (i.e., without averaging them). The secant method was employed to estimate the parameters by minimizing the Chi-square values between measured and modelled values, and standard errors were calculated to assess parameter uncertainty. The quality of fit between experimental and simulated data was assessed by calculating Theil's Inequality Coefficient (TIC, Eq. (7) (Decostere et al., 2016), where a TIC value lower than 0.3 demonstrates a good agreement between model simulations and experimental measurements (Coppens et al., 2014).

$$TIC = \frac{\sqrt{\sum_i \left(y_{i,s} - y_{i,m}\right)^2}}{\sqrt{\sum_i y_{i,s}^2} + \sqrt{\sum_i y_{i,m}^2}} \tag{7}$$

where $y_{i,s}$ is the simulated value for variably y and $y_{i,m}$ is the measured data point.

2.8. Model-based scenario analysis

The validated model can be used to improve the design and operation of PPB-based PBR systems. A scenario analysis was conducted with a fixed illuminated surface area of 1 m^2, varying PBR reactor thickness values from 1 to 30 cm, and HRTs of 1, 2, and 4 d. The PBR volume and flow rate were adjusted accordingly to ensure consistency with the set HRT values. The PBR operation under different conditions was simulated for a duration of 30 d to assess the impact of these parameters on biomass productivity, biomass concentration, and residual substrate concentration at steady state. These indicators were used to identify optimal combinations of reactor thickness and HRT that enhance light utilization and reactor performance.

3. Results and discussion

3.1. Purple phototrophic bacteria mixed culture characterization

Microbial community characterization confirmed the presence of PPB in every batch growth sample. The overall bacterial composition across the different light intensity conditions is illustrated in Fig. 1. The samples clustered according to the applied incident light intensity conditions, highlighting that some differences in bacterial community due to light conditions were considerable, although the abundance of PPB was higher than 75 % in all the samples. *Rhodopseudomonas* sp. and *Rhodobacter* sp. dominated the overall microbial communities, with their relative abundances slightly varying between conditions. The experimental data indicated that 10 W·m^{-2} was the optimal light intensity for the growth of *Rhodopseudomonas* sp., as it exhibited the highest relative abundance under this condition (see Supplementary Material). In contrast, *Rhodobacter* sp. exhibited a different response, demonstrating a more pronounced increase in the abundance at 40 W·m^{-2} (see Supplementary Material). The differences in the photosynthetic apparatus between the two genera likely explain these observations. *Rhodopseudomonas* sp. possess a more diverse photosynthetic system, featuring several types of light harvesting (LH) complexes (e.g., LH2, LH3, and LH4), which allow for significant adaptability to varying light intensities (Fixen et al., 2016). In addition to light-harvesting complexes, differences in pigment composition between the two genera may influence their light adaptation strategies. *Rhodobacter* sp. predominantly utilize bacteriochlorophyll *a* and are distinguished by high intracellular concentration of carotenoids, such as spheroidene and spheroidenone, which play a critical role in photoprotection and light-harvesting. These adaptations allow *Rhodobacter* sp. to thrive under high-light conditions by mitigating photodamage and enhancing energy dissipation (Yeliseev et al., 1996). It is important to note that our experimental design focused on the immediate response of a single culture that had no prior exposure to high light intensities. This setup was designed to capture the short-term effects of light stress, rather than the longer-term adaptive responses. While it has been reported for *Rhodopseudomonas* sp. the acclimation over time through enrichment or repeated exposure to higher light intensities, gradually optimizing its photosynthetic systems to better cope with photoinhibition and enhance

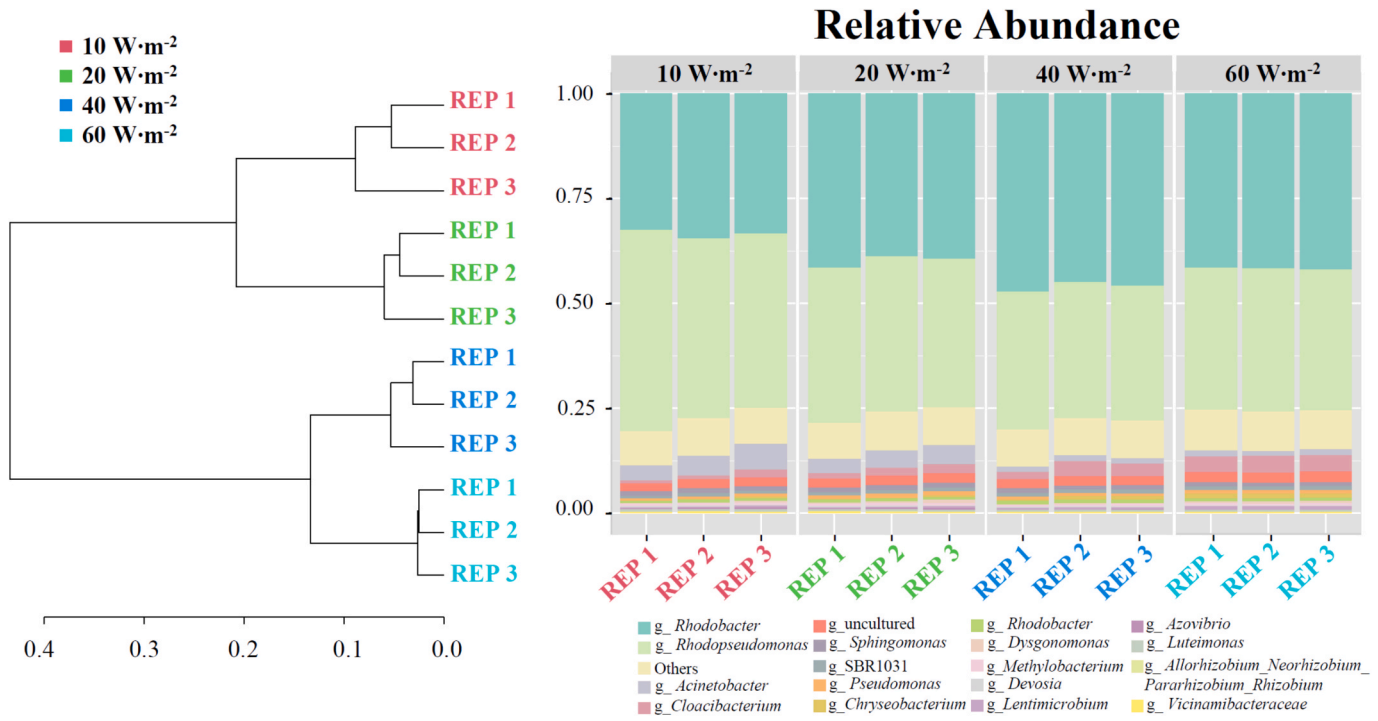

Fig. 1. Relative abundance of bacterial communities grown under light intensities of 10, 20, 40, and 60 W·m^{-2}. The dendrogram (left) shows sample clustering by similarity; the bar chart (right) displays the top 18 genera, with taxa below 5 % grouped as "Others".

efficiency under prolonged high-light conditions, such adaptation lies outside the scope of this study (Muzziotti et al., 2016; Tec-Campos et al., 2023).

Regarding biodiversity indexes, the α-diversity, representing the richness and evenness within each sample, was evaluated using Simpson's index and showed no statistically significant differences with varying light intensity (ANOVA, F = 3.4849, p = 0.0701) (see Supplementary Material). On the other hand, β-diversity, which measures the variation in community composition between samples, was more significantly influenced by light intensity conditions (see Supplementary

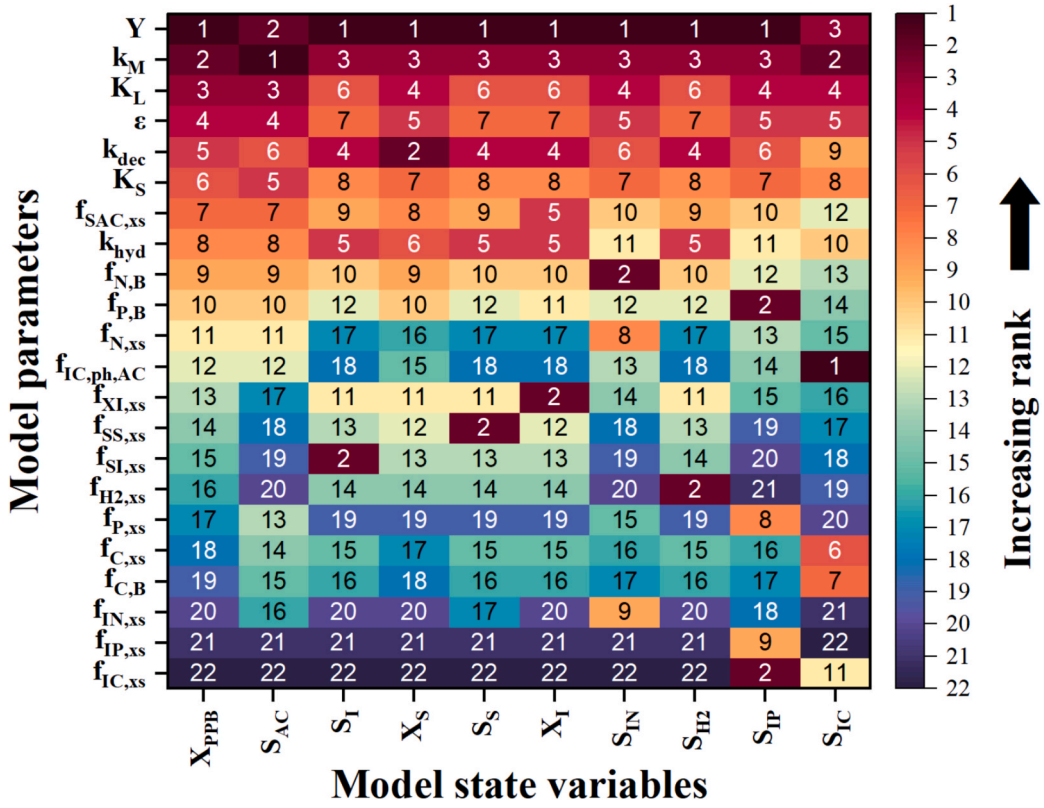

Fig. 2. Ranking of the model parameters across the model state variables assessed in sensitivity analysis.

Material, F = 18.618, R^2 = 0.87471, p = 0.001).

3.2. Purple phototrophic bacteria mixed culture modelling

3.2.1. Sensitivity analysis

As introduced earlier, the existing PAnM model (Puyol et al., 2017) was simplified and modified to include a light dependency function for PPB, allowing for the representation of light attenuation and facilitating parameter estimation. While Beer-Lambert law is effective in describing light attenuation profiles for PPB systems (Capson-Tojo et al., 2022), it is worth noting that it can overestimate the energy absorbed by each layer inside the PBR at low biomass concentrations, since scattering is not properly modelled and its effect is then lumped in the absorption coefficient (Amini et al., 2025). Despite this drawback and the fact that integration of scattering-aware radiation transfer models into biokinetic models would be the most accurate solution, it has been shown that the percentage differences between average light intensities inside PBRs estimated using the Beer-Lambert law, compared to CFD simulations, remain within 0.15–16 % for biomass concentrations ranging from 40 to 320 mgTSS·L^{-1} (Amini et al., 2025). At higher PPB concentrations, the difference between this model and more accurate ones, such as CFD, tends to be less pronounced. Therefore, given that this study reached concentrations higher than 1 g COD·L^{-1}, the Beer-Lambert law was used, as it is the simplest and most widely accepted approach for representing light attenuation in phototrophic models.

As shown in Fig. 2, sensitivity analysis was preliminarily carried out to identify the most relevant model parameters, which were then subjected to calibration. Among all model parameters, the PPB growth yield (Y), the maximum uptake rate of acetate (k_M), half-saturation of light (K_L), the light extinction coefficient (ε), and some relevant parameters related to bacterial kinetics and substrate characterization, such as the half-saturation constant for acetate (K_S) and the decay rate constant of PPB (k_{dec}), were the most sensitive parameters.

3.2.2. Parameter estimation

Based on the sensitivity analysis outcomes, the first six ranked parameters were chosen as the most influential. Three parameters of k_M, K_L, and k_{dec} were then subjected to estimation, with the results presented in Table 3. The biomass yield for each experiment was calculated as described in Section 2.4, resulting in an average value of 0.96 ± 0.02 mg COD·mg COD^{-1}. Moreover, the experimentally measured ε values from our previous work were used in the model, as described in Section 2.6. It should be noted that the other parameters involved in the model remained at the nominal values reported for the PAnM model by Puyol et al. (2017).

The k_M value obtained in this study (3.82 ± 0.33 mg COD·mg COD^{-1}·d^{-1}) was higher than those reported by Puyol et al. (2017) and Capson-Tojo et al. (2023) (2.40–2.73 mg COD·mg COD^{-1}·d^{-1}). This variation could be attributed to differences in light intensity, microbial community, or experimental conditions, including substrate concentration ranges. The estimated K_L value (3.16 ± 1.06 W·m^{-2}) in this study was in line with the one reported by Capson-Tojo et al. (2022), which was 4.58 ± 7.40 W·m^{-2}. Moreover, the k_{dec} value has been previously reported to range from 0.01 to 0.09 d^{-1} (Alloul et al., 2023; Puyol et al., 2017), which is consistent with the value estimated in this study.

Based on the literature studies for pure PPB cultures, it has been also reported that light intensity would result in photo-inhibition (Ross and Pott, 2022; Shi and Yu, 2005; Zhou et al., 2014). To further explore the possible photo-inhibition by higher light intensity for mixed PPB cultures, an additional batch experiment under incident light intensity of 85 W·m^{-2} was conducted. However, the results did not reveal any photo-inhibition as the biomass growth did not decline (see Supplementary Material) unlike the results observed by Shi and Yu (2005), that found the cell growth significantly declined when the light intensity exceeded 5000 lx (~ 39.5 W·m^{-2}). It is worth mentioning that while the incident light intensity is a useful parameter for standardizing experiments, it does not provide complete information about light environment within the culture. The incident light intensity provides a baseline measurement, but the actual light intensity that causes photo-inhibition can vary depending on how much light is absorbed by the cells.

Table 3
Estimated model parameters (value ± standard error).

Parameter	Unit	Value
k_M	mg COD·mg COD^{-1}·d^{-1}	3.82 ± 0.33
K_L	W·m^{-2}	3.16 ± 1.06
k_{dec}	d^{-1}	0.02 ± 0.03

3.2.3. Model performance

The comparison of the experimental data with model predictions for the experiments under different light intensity conditions is reported in Fig. 3(a)–(d), showing that the implementation of the combined light extinction and biokinetic model proposed in this study allowed for the accurate prediction of the experimental biomass and substrate concentrations across all tested incident light intensities. It should be noted that preliminary simulations that did not consider light attenuation could describe the observed data trend like the ones shown in Fig. 3(a)–(d). However, the estimated parameters were not realistic, as light

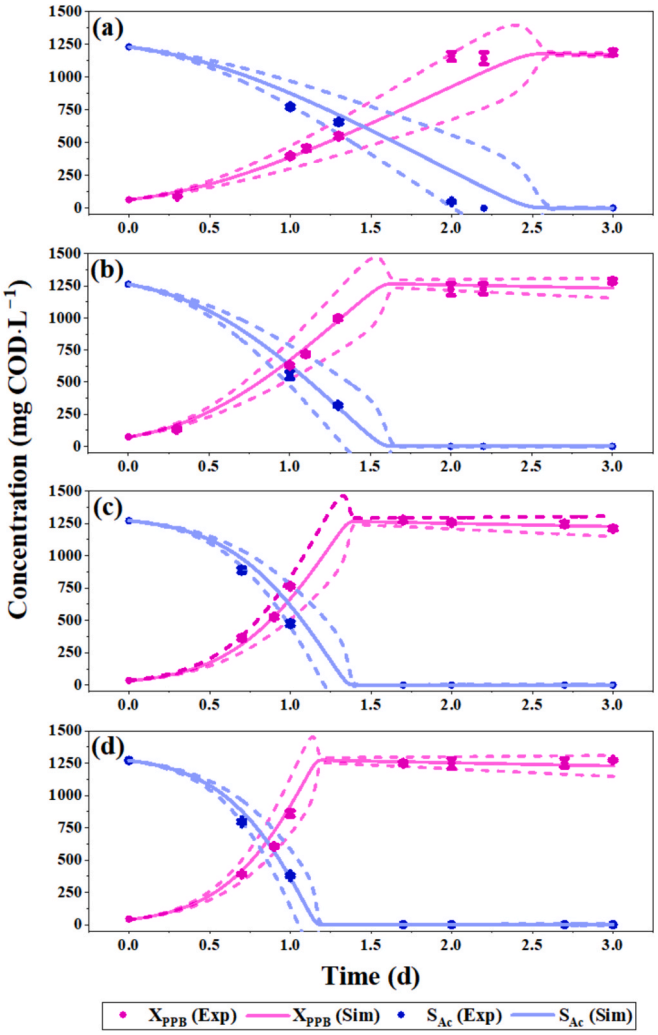

Fig. 3. Experimental (dots) and modelled (continuous lines) values obtained for the biomass (purple) and substrate (blue) concentrations at different light intensities: (a) 10 W·m^{-2}, (b) 20 W·m^{-2}, (c) 40 W·m^{-2}, and (d) 60 W·m^{-2}. Dashed lines represent the estimated error bounds.

attenuation does occur in PPB mixed cultures. In a similar context, Puyol et al. (2017) modelled PPB growth using the incident light intensity without accounting for light attenuation and succeeded in fitting the experimental data. While the estimated k_M appeared reasonable, the K_L value was notably high. This contrasts with the findings of this study and those reported by Capson-Tojo et al. (2022), which highlights the importance of incorporating light attenuation to obtain realistic kinetic parameters. Therefore, PPB modelling should carefully consider light attenuation effects to ensure accurate parameter estimation and reliable model predictions, particularly under varying light conditions and/or varying biomass concentrations. Moreover, in systems operating under variable outdoor light conditions, implementing variable extinction coefficients would possibly require dynamic recalibration strategies that account for photoadaptation, seasonal fluctuations, and microbial community shifts. Addressing it would require a more detailed characterization of biomass pigments and potentially other factors such as influent medium turbidity or color (Rossi et al., 2025). These aspects are critical for ensuring model reliability in real-world scenarios and represent important avenues for future research.

When analyzing the experimental data, it is evident that biomass concentrations followed the typical trend expected in batch growth tests, in which the biomass grows exponentially until reaching a plateau, after which the growth becomes limited by substrate availability. During all the tests, the biomass concentration reached maximum values of 1190–1290 mg COD·L^{-1}, while the substrate was completely consumed within 30 to 48 h. Overall, the goodness of fit for the proposed model was well demonstrated by the obtained TIC values, which were well below the threshold proposed as an indicator of good agreement with experimental data (Coppens et al., 2014). The calculated TIC values were in the range of 0.02–0.06 for the PPB concentration and ranged from 0.02 to 0.09 for substrate concentrations at different tested incident light intensities (Table 4).

3.3. Model validation using a semi-continuous flat-plate photobioreactor

To validate the kinetic parameters estimated from batch experiments, a PBR operated in semi-continuous mode at 40 W·m^{-2} was simulated using the obtained values. The estimated parameters, including k_M, K_L, and k_{dec} were directly applied to the continuous system modelling. This approach aimed to assess whether the batch-derived values could accurately predict PPB growth and substrate consumption under continuous conditions.

As shown in Fig. 4, the model accurately captured the biomass growth and substrate consumption trends, demonstrating good agreement with the experimental data. During the initial phase, a rapid increase in PPB biomass was observed, followed by stabilization as steady-state conditions were reached. Similarly, acetate concentrations declined sharply in the early phase, stabilizing at low concentrations. Minor discrepancies between experimental and simulated values can be attributed to operational variations. Overall, the results confirm that the kinetic parameters estimated from batch experiments reliably predict PPB growth and substrate concentrations in a continuous system, with TICs of 0.03 for biomass and 0.06 for substrate, requiring no further parameter adjustments.

Table 4
TIC values obtained for PPB and substrate concentrations for the tests performed at different incident light intensities.

Light intensity (W·m^{-2})	TIC value (−)	
	PPB concentration	Substrate concentration
10	0.06	0.09
20	0.02	0.02
40	0.02	0.05
60	0.03	0.03

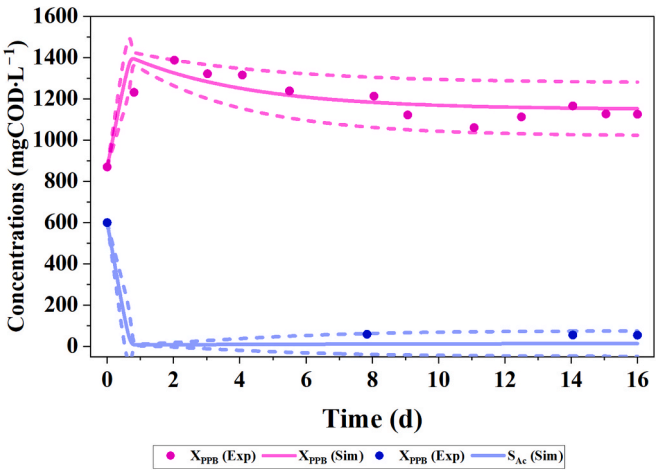

Fig. 4. Model validation in a semi-continuous flat-plate PBR at 40 W·m^{-2}. Experimental (dots) and modelled (continuous lines) values obtained for the biomass (purple) and substrate (blue) concentrations. Dashed lines represent the estimated error bounds.

3.4. Process insights from purple phototrophic mixed cultures modelling

A model-based scenario analysis was conducted to evaluate the impact of the reactor thickness and HRT on biomass productivity as well as biomass and substrate concentrations at the steady-state conditions under continuous-mode operation. A flat plate PBR was considered, with an illuminated surface area of 1 m^2 and varying PBR thickness (H = 1 to 30 cm). Various HRT values were considered (1, 2, and 4 d). The PBR volume and flow rate were adjusted case-by-case to ensure the simulated operating conditions.

As shown in Fig. 5, the results deduced from the model highlight the critical role of reactor thickness and HRT in defining PBR efficiency. By analyzing trends at HRT = 1 d, an increase in areal productivity is observed with increasing thickness, reflecting the fact that when H increases, the PBR volume increases as well, which in turn results in an increase in inflow rate and thus in organic load per unit of surface, eventually increasing substrate availability and productivity. This is confirmed by the increasing effluent COD concentration when increasing H from 1 to 5 cm. Further increase in H leads to significant increase in effluent COD concentration, suggesting that the organic load overcomes the PBR conversion capacity, which is in accordance with a stable areal productivity for H > 10 cm. Thus, at HRT = 1 d, organic availability is limiting for H < 10 cm, while light becomes the limiting factor for H > 10 cm. For H > 10 cm, light energy is fully used and areal productivity stabilized, so that volumetric productivity and biomass concentration decrease because of the larger dilution associated with the increasing reactor volume. When the HRT increases, the effect of H increase on productivity is similar, but the minimum value of H after which organic availability ceases to play a limiting role increases, being H > 15 cm for an HRT of 2 d and H > 30 cm for an HRT of 4 d. Indeed, at HRT of 4 d, organic load remains limiting even at H = 30 cm, as demonstrated by the low residual COD in the effluent. However, the longer residence time allows a more effective biomass conversion, thus achieving higher areal productivity at increasing HRT under non limiting substrate availability. Volumetric productivity remains constant until light becomes the limiting factor. Indeed, under light limitation, increasing volume reduces the volumetric productivity since the areal productivity remains the same while reactor volume increases. These types of analyses allow for defining ideal design conditions once the PBR goals are established. Increasing HRT and H enhances biomass productivity, but it leads to higher capital costs (due to the larger volume) and operational costs (resulting from the higher organic load and lower COD conversion efficiency). Thus, a trade-off must be found by a

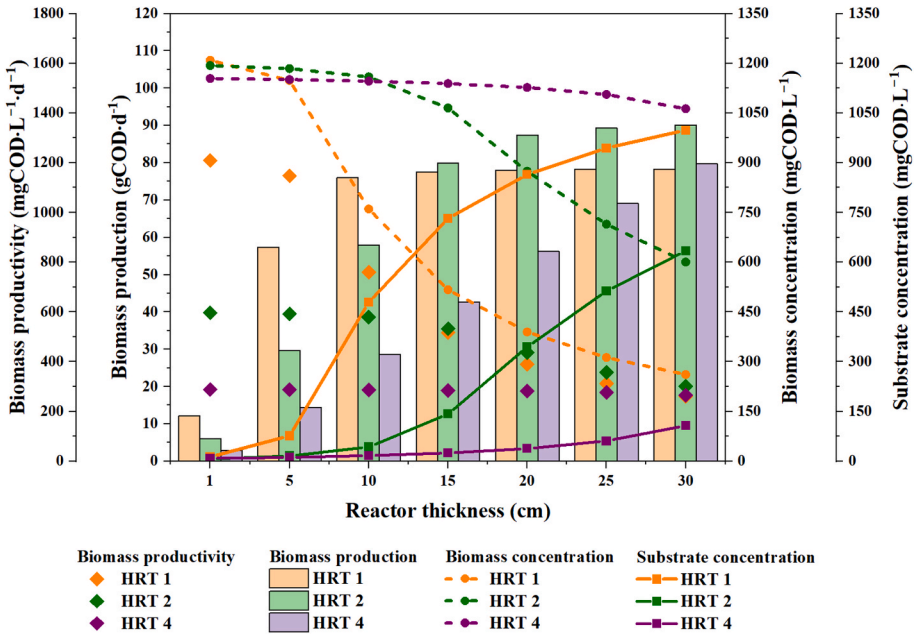

Fig. 5. Effect of reactor thickness and HRT on biomass productivity, biomass concentration, and substrate concentration in a continuous flat-plate PBR under a light intensity of 40 $W \cdot m^{-2}$.

comprehensive cost analysis.

4. Conclusions

This study investigated the effect of light intensity on the growth kinetics of a PPB mixed culture through lab-scale experiments which were used to calibrate a Monod-type mechanistic model. The model showed good performance for all the tested light intensity conditions, being able to describe light limitations, and it was validated on a continuous flow PBR. This resulted in an acetate uptake rate of 3.82 ± 0.33 mg COD·mg $COD^{-1} \cdot d^{-1}$ and a half saturation coefficient of 3.16 ± 1.06 $W \cdot m^{-2}$. Microbial characterization revealed that PPB abundance was higher than 75 % in all the samples, with light significantly influencing bacterial community structure. *Rhodopseudomonas* sp. had the highest relative abundance at 10 $W \cdot m^{-2}$, while *Rhodobacter* sp. thrived at higher light intensities, particularly at 40 $W \cdot m^{-2}$, indicating distinct microbial responses to light variations despite a stable PPB presence. The model-based scenario analysis also emphasized the critical role of reactor thickness and HRT.

CRediT authorship contribution statement

Ali Amini: Writing – original draft, Visualization, Validation, Software, Methodology, Investigation, Formal analysis, Data curation, Conceptualization. **Simone Rossi:** Writing – review & editing, Validation, Software, Methodology, Formal analysis, Data curation. **Valiallah Amirian Mojarad:** Writing – review & editing, Validation, Investigation. **Gabriele Bellotti:** Methodology, Data curation. **Fabrizio Cappa:** Supervision, Methodology. **Filippo Vaccari:** Software, Methodology, Data curation. **Edoardo Puglisi:** Funding acquisition. **Roberto Canziani:** Writing – review & editing, Validation. **Elena Ficara:** Writing – review & editing, Validation, Methodology, Formal analysis, Conceptualization. **Andrea Turolla:** Writing – review & editing, Validation, Supervision, Resources, Project administration, Methodology, Funding acquisition, Formal analysis, Conceptualization.

Declaration of competing interest

The authors declare the following financial interests/personal relationships which may be considered as potential competing interests: Andrea Turolla reports financial support was provided by Italian Ministry of University and Research. If there are other authors, they declare that they have no known competing financial interests or personal relationships that could have appeared to influence the work reported in this paper.

Acknowledgements

The research work was partially funded by the PRIN 2022 “PHARPLE” project (ID 2022MHBMEH) funded by the Italian MUR, and the Agritech National Research Center (Task 8.3.2) funded by the European Union Next-GenerationEU (PIANO NAZIONALE DI RIPRESA E RESILIENZA (PNRR) – MISSIONE 4 COMPONENTE 2, INVESTIMENTO 1.4 – D.D. 1032 17/06/2022, CN00000022). The authors would like to gratefully thank the COST ACTION “PURPLEGAIN” (CA21146) funded by the European Union for the training and networking resources made available to the research group.

Appendix A. Supplementary data

Supplementary data to this article can be found online at https://doi.org/10.1016/j.biortech.2025.132873.

Data availability

Data will be made available on request.

References

Alloul, A., Moradvandi, A., Puyol, D., Molina, R., Gardella, G., Vlaeminck, S.E., De Schutter, B., Abraham, E., Lindeboom, R.E.F., Weissbrodt, D.G., 2023. A novel mechanistic modelling approach for microbial selection dynamics: Towards improved design and control of raceway reactors for purple bacteria. Bioresour. Technol. 390, 129844. https://doi.org/10.1016/J.BIORTECH.2023.129844.

Amini, A., Porciatti, E., Minotto, A., Moranchel, T., Sassella, A., Canziani, R., Turolla, A., 2025. Exploring optical properties and radiation transfer in a mixed culture of purple phototrophic bacteria grown in a flat-plate photobioreactor via combined experimental and modelling approach. J. Environ. Chem. Eng. 13, 115425. https://doi.org/10.1016/J.JECE.2025.115425.

Bartram, A.K., Lynch, M.D.J., Stearns, J.C., Moreno-Hagelsieb, G., Neufeld, J.D., 2011. Generation of multimillion-sequence 16S rRNA gene libraries from complex

microbial communities by assembling paired-end illumina reads. Appl. Environ. Microbiol. 77, 3846–3852. https://doi.org/10.1128/AEM.02772-10.
Bernard, O., Rémond, B., 2012. Validation of a simple model accounting for light and temperature effect on microalgal growth. Bioresour. Technol. 123, 520–527. https://doi.org/10.1016/J.BIORTECH.2012.07.022.
Berry, D., Ben Mahfoudh, K., Wagner, M., Loy, A., 2011. Barcoded primers used in multiplex amplicon pyrosequencing bias amplification. Appl. Environ. Microbiol. 77, 7846–7849. https://doi.org/10.1128/AEM.05220-11.
Capson-Tojo, G., Batstone, D.J., Grassino, M., Hülsen, T., 2022. Light attenuation in enriched purple phototrophic bacteria cultures: Implications for modelling and reactor design. Water Res. 219, 118572. https://doi.org/10.1016/J.WATRES.2022.118572.
Capson-Tojo, G., Batstone, D.J., Grassino, M., Vlaeminck, S.E., Puyol, D., Verstraete, W., Kleerebezem, R., Oehmen, A., Ghimire, A., Pikaar, I., Lema, J.M., Hülsen, T., 2020. Purple phototrophic bacteria for resource recovery: challenges and opportunities. Biotechnol. Adv. 43, 107567. https://doi.org/10.1016/J.BIOTECHADV.2020.107567.
Capson-Tojo, G., Batstone, D.J., Hülsen, T., 2023. Expanding mechanistic models to represent purple phototrophic bacteria enriched cultures growing outdoors. Water Res. 229, 119401. https://doi.org/10.1016/J.WATRES.2022.119401.
Carvalho, A.P., Silva, S.O., Baptista, J.M., Malcata, F.X., 2011. Light requirements in microalgal photobioreactors: an overview of biophotonic aspects. Appl. Microbiol. Biotechnol. 89, 1275–1288. https://doi.org/10.1007/s00253-010-3047-8.
Casagli, F., Zuccaro, G., Bernard, O., Steyer, J.P., Ficara, E., 2021. ALBA: a comprehensive growth model to optimize algae-bacteria wastewater treatment in raceway ponds. Water Res. 190, 116734. https://doi.org/10.1016/J.WATRES.2020.116734.
Cerruti, M., Kim, J.-H., Pabst, M., Loosdrecht, M.C.M.V., Weissbrodt, D.G., 2022. Light intensity defines growth and photopigment content of a mixed culture of purple phototrophic bacteria. Front. Microbiol. 13, 1014695. https://doi.org/10.3389/FMICB.2022.1014695.
Collins, W.D., Lee-Taylor, J.M., Edwards, D.P., Francis, G.L., 2006. Effects of increased near-infrared absorption by water vapor on the climate system. J. Geophys. Res. Atmos. 111, 18109. https://doi.org/10.1029/2005JD006796.
Coppens, J., Decostere, B., Van Hulle, S., Nopens, I., Vlaeminck, S.E., De Gelder, L., Boon, N., 2014. Kinetic exploration of nitrate-accumulating microalgae for nutrient recovery. Appl. Microbiol. Biotechnol. 98, 8377–8387. https://doi.org/10.1007/S00253-014-5854-9.
Dalaei, P., Bahreini, G., Nakhla, G., Santoro, D., Batstone, D., Hülsen, T., 2020. Municipal wastewater treatment by purple phototropic bacteria at low infrared irradiances using a photo-anaerobic membrane bioreactor. Water Res. 173, 115535. https://doi.org/10.1016/J.WATRES.2020.115535.
Damergi, E., Qin, P., Sharma, S., Nazeeruddin, M.K., Ludwig, C., 2021. Enhancing Algae Biomass Production by Using Dye-Sensitized Solar Cells as Filters. https://doi.org/10.1021/acssuschemeng.1c03780.
Decostere, B., De Craene, J., Van Hoey, S., Vervaeren, H., Nopens, I., Van Hulle, S.W.H., 2016. Validation of a microalgal growth model accounting with inorganic carbon and nutrient kinetics for wastewater treatment. Chem. Eng. J. 285, 189–197. https://doi.org/10.1016/J.CEJ.2015.09.111.
Delamare-Deboutteville, J., Batstone, D.J., Kawasaki, M., Stegman, S., Salini, M., Tabrett, S., Smullen, R., Barnes, A.C., Hülsen, T., 2019. Mixed culture purple phototrophic bacteria is an effective fishmeal replacement in aquaculture. Water Res. X 4, 100031. https://doi.org/10.1016/J.WROA.2019.100031.
Fixen, K.R., Oda, Y., Harwood, C.S., 2016. Clades of Photosynthetic Bacteria Belonging to the Genus Rhodopseudomonas Show Marked Diversity in Light-Harvesting Antenna Complex Gene Composition and Expression . mSystems 1. https://doi.org/10.1128/MSYSTEMS.00006-15.
García, D., de Godos, I., Domínguez, C., Turiel, S., Bolado, S., Muñoz, R., 2019. A systematic comparison of the potential of microalgae-bacteria and purple phototrophic bacteria consortia for the treatment of piggery wastewater. Bioresour. Technol. 276, 18–27. https://doi.org/10.1016/J.BIORTECH.2018.12.095.
Golomysova, A., Gomelsky, M., Ivanov, P.S., 2010. Flux balance analysis of photoheterotrophic growth of purple nonsulfur bacteria relevant to biohydrogen production. Int. J. Hydrogen Energy 35, 12751–12760. https://doi.org/10.1016/J.IJHYDENE.2010.08.133.
Hädicke, O., Grammel, H., Klamt, S., 2011. Metabolic network modeling of redox balancing and biohydrogen production in purple nonsulfur bacteria. BMC Syst. Biol. 5, 1–18. https://doi.org/10.1186/1752-0509-5-150.
Hülsen, T., Batstone, D.J., Keller, J., 2014. Phototrophic bacteria for nutrient recovery from domestic wastewater. Water Res. 50, 18–26. https://doi.org/10.1016/J.WATRES.2013.10.051.
Kaewsuk, J., Thorasampan, W., Thanuttamavong, M., Seo, G.T., 2010. Kinetic development and evaluation of membrane sequencing batch reactor (MSBR) with mixed cultures photosynthetic bacteria for dairy wastewater treatment. J. Environ. Manage. 91, 1161–1168. https://doi.org/10.1016/J.JENVMAN.2010.01.012.
Lee, E., Jalalizadeh, M., Zhang, Q., 2015. Growth kinetic models for microalgae cultivation: a review. Algal Res. 12, 497–512. https://doi.org/10.1016/J.ALGAL.2015.10.004.
Liu, S., Li, X., Zhang, G., Zhang, J., 2015. Effect of magnesium ion on crt gene expression in improving carotenoid yield of Rhodobacter sphaeroides. Arch. Microbiol. 197, 1101–1108. https://doi.org/10.1007/s00203-015-1150-z.
Liu, S., Zhang, G., Zhang, J., Li, X., Li, J., 2016. Performance, carotenoids yield and microbial population dynamics in a photobioreactor system treating acidic wastewater: effect of hydraulic retention time (HRT) and organic loading rate (OLR). Bioresour. Technol. 200, 245–252. https://doi.org/10.1016/J.BIORTECH.2015.10.044.
Lu, Y., Zhou, G., Ewald, J., Pang, Z., Shiri, T., Xia, J., 2023. MicrobiomeAnalyst 2.0: comprehensive statistical, functional and integrative analysis of microbiome data. Nucleic Acids Res. 51, W310–W318. https://doi.org/10.1093/NAR/GKAD407.
Martínez, C., Mairet, F., Bernard, O., 2018. Theory of turbid microalgae cultures. J. Theor. Biol. 456, 190–200. https://doi.org/10.1016/J.JTBI.2018.07.016.
Muzziotti, D., Adessi, A., Faraloni, C., Torzillo, G., De Philippis, R., 2016. H2 production in Rhodopseudomonas palustris as a way to cope with high light intensities. Res. Microbiol. 167, 350–356. https://doi.org/10.1016/J.RESMIC.2016.02.003.
Ormerod, J.G., Ormerod, K.S., Gest, H., 1961. Light-dependent utilization of organic compounds and photoproduction of molecular hydrogen by photosynthetic bacteria; relationships with nitrogen metabolism. Arch. Biochem. Biophys. 94, 449–463. https://doi.org/10.1016/0003-9861(61)90073-X.
Prachanurak, P., Chiemchaisri, C., Chiemchaisri, W., Yamamotob, K., 2014. Biomass production from fermented starch wastewater in photo-bioreactor with internal overflow recirculation. Bioresour. Technol. 165, 129–136. https://doi.org/10.1016/J.BIORTECH.2014.03.119.
Puyol, D., Barry, E.M., Hülsen, T., Batstone, D.J., 2017. A mechanistic model for anaerobic phototrophs in domestic wastewater applications: photo-anaerobic model (PAnM). Water Res. 116, 241–253. https://doi.org/10.1016/J.WATRES.2017.03.022.
Reichert, P., 1994. AQUASIM – a tool for simulation and data analysis of aquatic systems. Water Sci. Technol. 30, 21–30. https://doi.org/10.2166/WST.1994.0025.
Ross, B.S., Pott, R.W.M., 2022. Investigating and modeling the effect of light intensity on Rhodopseudomonas palustris growth. Biotechnol. Bioeng. 119, 907–921. https://doi.org/10.1002/BIT.28026.
Rossi, S., Capson-Tojo, G., Sanchez-Zurano, A., Carecci, D., Batstone, D.J., Acien-Fernandez, G., Ficara, E., 2025. Recent advances and challenges in mechanistic modelling of photosynthetic processes for wastewater treatment. Water Res. 278, 123216. https://doi.org/10.1016/J.WATRES.2025.123216.
Shi, X.Y., Yu, H.Q., 2005. Response surface analysis on the effect of cell concentration and light intensity on hydrogen production by Rhodopseudomonas capsulata. Process Biochem. 40, 2475–2481. https://doi.org/10.1016/J.PROCBIO.2004.09.010.
Solimeno, A., Samsó, R., Uggetti, E., Sialve, B., Steyer, J.P., Gabarró, A., García, J., 2015. New mechanistic model to simulate microalgae growth. Algal Res. 12, 350–358. https://doi.org/10.1016/J.ALGAL.2015.09.008.
Tec-Campos, D., Posadas, C., Tibocha-Bonilla, J.D., Thiruppathy, D., Glonek, N., Zuñiga, C., Zepeda, A., Zengler, K., 2023. The genome-scale metabolic model for the purple non-sulfur bacterium Rhodopseudomonas palustris Bis A53 accurately predicts phenotypes under chemoheterotrophic, chemoautotrophic, photoheterotrophic, and photoautotrophic growth conditions. PLoS Comput. Biol. 19, e1011371. https://doi.org/10.1371/JOURNAL.PCBI.1011371.
White, T., Bruns, T., Lee, S., 1990. Amplification and direct sequencing of fungal ribosomal RNA genes for phylogenetics. In: Innis, M.A., Gelfand, D.H. (Eds.), PCR Protocols: a Guide to Methods and Applications. Academic Press, London, pp. 315–322.
Yeliseev, A.A., Eraso, J.M., Kaplan, S., 1996. Differential carotenoid composition of the B875 and B800-850 photosynthetic antenna complexes in Rhodobacter sphaeroides 2.4.1: involvement of spheroidene and spheroidenone in adaptation to changes in light intensity and oxygen availability. J. Bacteriol. 178, 5877–5883. https://doi.org/10.1128/JB.178.20.5877-5883.1996.
Zhou, Q., Zhang, P., Zhang, G., 2014. Biomass and carotenoid production in photosynthetic bacteria wastewater treatment: effects of light intensity. Bioresour. Technol. 171, 330–335. https://doi.org/10.1016/J.BIORTECH.2014.08.088.